Luminescent nanoparticles of Mn doped ZnS passivated with sodium hexametaphosphate

H.C. Warad, S.C. Ghosh, B. Hemtanon, C. Thanachayanont & J. Dutta

Luminescent nanoparticles of Mn doped ZnS passivated with sodium hexametaphosphate

H.C. Warad[a], S.C. Ghosh[a], B. Hemtanon[a], C. Thanachayanont[b], J. Dutta[a],*

[a]*Microelectronics, School of Advanced Technologies, Asian Institute of Technology, P.O. Box 4, Klong Luang, Pathumthani 12120, Thailand*
[b]*National Metal and Materials Technology Center, 114 Thailand Science Park, Phaholyothin Road, Klong 1, Klong Luang, Pathumthani 12120, Thailand*

Abstract

We report the synthesis of luminescent nanoparticles of manganese doped zinc sulfide ($ZnS:Mn^{2+}$) with an emission peak at around 590 nm. Nanoparticles of $ZnS:Mn^{2+}$ are prepared by a co-precipitation reaction from homogenous solutions of zinc and manganese salts. Based on Ostwald ripening and surface passivation, we discuss a mechanism for the formation of $ZnS:Mn^{2+}$ nanoparticles. The reaction proceeds with the nucleation of ZnS crystals, which are immediately passivated by the anions in the solution. This in turn attracts cations including zinc and manganese which contribute to the growth of the crystal. These nanoparticles are sterically stabilized using polyphosphates of sodium namely sodium tripolyphosphate (STTP) and sodium hexametaphosphate (SHMP). The nanoparticles consist of particles of 60–80 nm in diameter, each containing primary crystallites that was estimated from the X-ray diffraction patterns to be at around 2.2 nm.

1. Introduction

Semiconductor nanocrystals are described as a state of matter that is intermediate between individual molecule and bulk [1]. Transition from bulk to nanoparticles lead to the display of quantum mechanical properties and an increased dominance of surface atoms which increases the chemical reactivity of a material. Notable examples include tunable bandgap [2] and catalytic behavior [3], respectively. The small size and high optical activity of certain semiconductors make them interesting for applications in disciplines ranging from optoelectronics [4], catalysis [5] to fluorescence microscopy [6].

Particles in nanometric sizes show unique physical properties, for example with the decrease of particle size, extremely high surface area to volume ratio is obtained leading to an increase in surface specific active sites for chemical reactions and photon absorption to enhance the reaction and absorption efficiency. The enhanced surface area increases surface states, which changes the activity of electrons and holes, affecting the chemical reaction dynamics. For instance, the size quantization can increase the bandgap of photocatalysts to enhance the redox potential of conduction band electrons and valence band holes [7]. Also, nanoparticles can induce the possibility of indirect electron transitions at the boundary of the crystals and realize the essential enhancement of light absorption.

The conventional approach for synthesis of nanoparticles involves chemical or physical attrition from bulk into objects of desired sizes and shapes (e.g. mechanical milling, ion implantation, etc.), and is referred as the 'top-down' approach. Inverse to the 'top-down' approach is a process universal in nature, involving the assembly of materials from molecular levels to form micro or macro-sized shapes and structures, often referred as 'bottom-up' approach or 'self-assembly' [8].

Wet chemical synthesis involving colloids is the most energy efficient 'bottom up' technique for the synthesis of nanoparticles. The chemical synthesis has the advantages of producing size-controlled, un-agglomerated nanoparticles.

---

* Corresponding author. Tel.: +66 2 524 5680; fax: +66 2 524 5697.
  E-mail address: joy@ait.ac.th (J. Dutta).

During synthesis of nanoparticles from a chemical reaction to form a colloidal system, upon addition of the reagents initially formed product molecules are called seeds. The number of seeds remains constant and over time; as more product molecules are formed the seeds grow in size in a thermodynamically controlled manner to form nano-crystallites [9]. Most of the physical or chemical properties exhibited by these nanoparticles are due to these crystallites. Further growth in size is due to these crystallites agglomerating to form primary particles. If this growth of particles is not controlled, then due to Ostwald ripening and van Der Waals interactions between particles, they agglomerate and settle down [10]. This agglomeration can be arrested by either stabilizing electrostatically or by inducing steric hindrances at appropriate stages in the precipitation reaction, to achieve size selective synthesis.

Electrostatic stabilization involves the creation of an electrical double layer arising from ions adsorbed on the surface and associated counter ions that surround the particle in the dispersing media. Thus, if the electric potential associated with the double layer is sufficiently high, columbic repulsion between the particles will prevent their agglomeration. Steric hindrance can be achieved by the adsorption of large molecules such as polymers on the surface of the particles. Two distinct effects describe this type of stabilization. First, the fact that the adsorbed molecules are restricted in motion causes a decrease in the configurational entropic contribution to the free energy. Second, the local increase in concentration of polymer chains between approaching particles results in an osmotic repulsion, since the solvent re-establishes equilibrium by diluting the polymer molecules, consequently separates the particles [8].

ZnS nanoparticles are often used as phosphors for display devices [11]. ZnS doped with manganese (orange red emission at around 590 nm) [12], copper (green emission at around 510 nm) [13] and silver (blue emission at around 440 nm) [14] have a potential application in field emission devices (FED) [15]. Semiconductor nanoparticles show effective photocatalysis property, e.g. in the artificial fixation of CO_2 [16]. It is believed that catalysis occurs on the surface of the particles. Cadmium sulfide (CdS) [17], zinc sulfide (ZnS) [17] and cadmium-rich cadmium selenide (CdSe) [16] of certain sizes act as efficient photocatalytic semiconductor nanoparticles. But CdS and CdSe are toxic and are also unstable undergoing photoanodic corrosion in aqueous media [18]. In this regard, the use of undoped ZnS nanocrystals could achieve similar results, and has the inherent advantage of being non-toxic also.

Organometallic method of synthesis of nanoparticles has been described by Bhargava et al. [19,20]. Yu et al. synthesized nanoparticles of $Zns:Mn^{2+}$ in methanol by using sodium polyphosphate as the capping agent [21]. Precipitations from homogeneous solutions have also been reported where it was found that particle size is a function of the nature of the associated anions [22,23]. Here, we describe the synthesis of $ZnS:Mn^{2+}$ nanoparticles using an organometallic to inorganic synthesis employing a co-precipitation reaction, and stabilized by steric hindrances by using polyphosphates of sodium namely sodium hexametaphosphate and sodium tripolyphosphate as capping agents.

2. Experimental

All synthesis was carried out in water for its inherent advantages of being simple and environment friendly. All steps of the synthesis were performed at room temperature and under ambient conditions.

Ten grams of sodium polyphosphate namely SHMP (Fluka Chemika) and STTP (Fluka Chemika) were separately dissolved in 70 cm^3 of De-ionized (DI) water and stirred. To each of this an aqueous solution of 0.25 M $Zn(CH_3COO)_2$ (Univar) and 1 mM $Mn(CH_3COO)_2$ (Fluka Chemika) was mixed together and stirred constantly and heated till boiling. After cooling to room temperature, 0.25 M sodium sulfide (Panreac) was added drop wise in an ice bath with constant stirring, resulting in formation of white precipitate of ZnS nanoparticles almost immediately. The supernatant was then centrifuged at 4000 rpm for 20 min to separate undesired agglomerates. In a few of the experiments, after washing the particles with de-ionized water the sample was freeze-dried to obtain fine powder of $ZnS:Mn^{2+}$ nanoparticles.

The sample characterizations were carried out using UV–Visible Spectroscopy (ELICO SL-164), Scanning Electron Microscope (JEOL, JSM-6301F), Fourier Transform Infrared Spectroscope (Perkin–Elmer), Fluorescence Spectroscope (Hitachi, F-4500 FL Spectrophotometer) and X-ray Diffraction (JEOL, JDX- 3530).

3. Results and discussions

Zinc acetate dissociates into zinc ions (Zn^{2+}) and acetate (Ac^-) ions in aqueous solution. Similarly, manganese acetate and sodium sulfide dissociate into their respective cations and anions. Sodium being more reactive than zinc and manganese, readily forms sodium acetate. Particles of ZnS nucleate due to the reaction between Zn^{2+} and S^{2-}, which subsequently grow by consuming more ions from the solution. The growth mechanism can be explained on the basis of Ostwald ripening [10]. Upon nucleation, the surface energy of the particles is very high and consequently the surface is passivated by adsorption of anions in the solution (Ac^- and S^{2-}). The accumulation of anions in turn attracts cations (Zn^{2+}, Mn^{2+} and Na^+) towards the surface of the particle. Zn^{2+} and Mn^{2+} react with S^{2-} and get incorporated into the crystal lattice of the nucleus (Fig. 1a). Eventually enough Na^+ accumulates (sodium is not known to form alloys with zinc [24]) to repulse Zn^{2+} ions from approaching the particle surface and the particle growth stops. These accumulated Na^+ ions form the stern
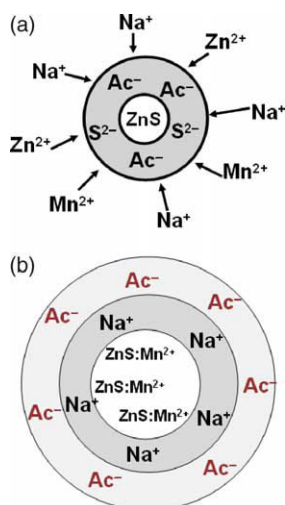
Fig. 1. (a) Simplified model of particles of ZnS nucleating due to reaction between Zn^{2+} and S^{2-} growing subsequently to form seeds. Due to high surface energy, surface is passivated with anions (S^{2-}, Ac^-), which in turn attract cations (Zn^{2+}, Mn^{2+}, Na^+) towards the surface of the particle. (b) Accumulated Na^+ ions forming a stern layer over ZnS nanoparticles, which due to positive charge attract Ac^- ions forming a diffusive layer, preventing initial agglomeration.

layer over ZnS nanoparticles, attracting Ac^- ions to form a diffuse layer over it (Fig. 1b). In this way, the particle growth is completely stopped. To avoid further agglomeration, a repulsive force must be added between the particles to balance the attractive forces. This is achieved by adsorbing a layer of polymer over nanoparticles inducing steric hindrance by employing STTP and SHMP as the stabilizing agent. The primary difference between the two polymers used was in the percentage of phosphorus pentaoxide (P_2O_5) content, sequestrating capabilities and the chain length. A series of experiments were conducted by changing the amount of each stabilizing agent to establish the most suitable conditions for obtaining non-agglomerating primary particles.

In Fig. 2, absorption spectra of SHMP capped ZnS:Mn^{2+} has been plotted, showing that the absorption edge increases

from 250 to 285 nm with a change in SHMP concentration from 0.5 to 12 g. From theory, the blue shift in the absorption edge is a measure of increasing bandgap that can be attributed to the presence of smaller crystallites due to quantum confinement effects. Further increase in SHMP from 10 to 12 g did not affect the crystallite size. This suggests that the capping agents also participate in the formation of ZnS crystallites. But in case of STTP, the absorption edge (Fig. 3) varies from 252 to 265 nm and are very close (except in case of 0.5 g), indicating that STTP is not as effective as SHMP to passivate particles.

It was noticed that for low concentrations of STPP, the solution turns white as soon as zinc acetate is added to it which is probably due to the formation of zinc hydroxide, which is white in color and/or larger agglomerates resulting in Mie scattering. But as the concentration of STPP is increased, the solution becomes less white and ultimately clear even after addition of zinc acetate. This effect can be explained on the basis of the sequestrating capability of the stabilizing agent which can be defined as the ability to disperse and form water soluble complexes with a variety of cations and to prevent them from precipitating. In case of SHMP, this effect is not as pronounced as it is found with STTP and for the same amount of solute in water, the solution turns less white after zinc acetate is added to it. Because of these advantages of SHMP over STTP, it was the preferred stabilizing agent in the synthesizing the Q-dots of ZnS: Mn^{2+}.

A typical Scanning Electron Micrograph (SEM) of ZnS:Mn^{2+} nanoparticles (Fig. 4) shows that particles have smooth surfaces due to the surface passivation with polymer and the average agglomerate size of around 60–80 nm. Fig. 5 shows the X-ray powder diffractogram of nanocrystalline ZnS doped with Mn^{2+} prepared with 10 g SHMP reveals that these quantum dots of ZnS:Mn^{2+} have zinc blende structure with planes at {111}, {220} and {311}, respectively. The XRD peaks are broadened due to the nanocrystalline nature of particles. These nanocrystals have lesser lattice planes compared to bulk, which
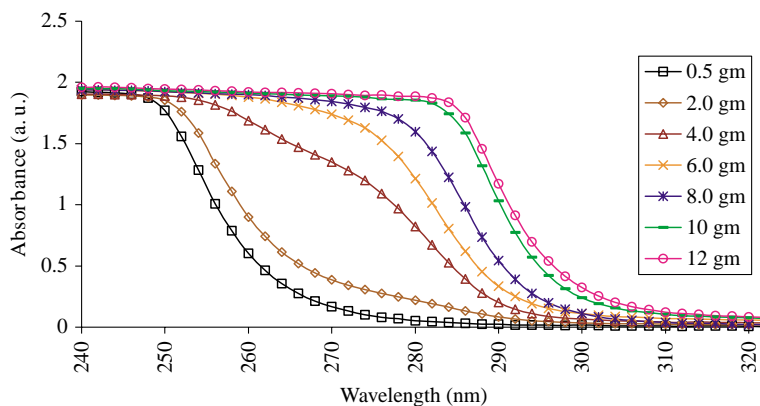

Fig. 2. Absorption spectra of ZnS nanoparticles synthesized with varying amounts of stabilizing agent SHMP, showing the absorption edge increasing from 250 to 285 nm with change from 0.5 to 12 g of SHMP content.
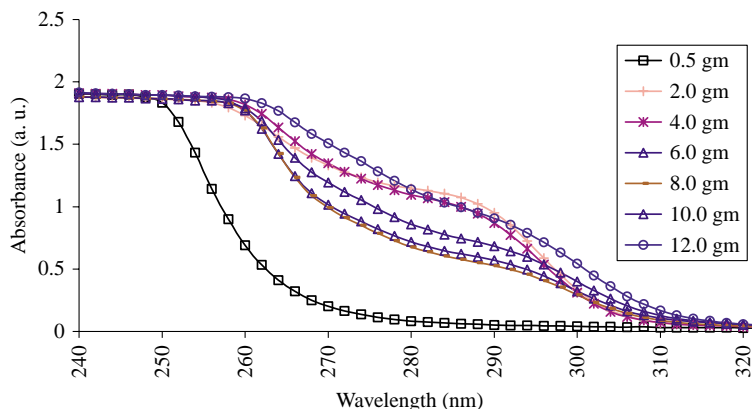
Fig. 3. Absorption spectra of ZnS nanoparticles synthesized with varying amounts of stabilizing agent SHMP, showing the absorption edge increasing from 252 to 265 nm with change from 0.5 to 12 g of STTP content.

contributes to the broadening of the peaks in the diffraction pattern. This broadening of the peak could also arise due to the micro-straining of the crystal structure arising from defects like dislocation and twinning, etc. These defects are believed to be associated with the chemically synthesized nanocrystals as they grow spontaneously during chemical reaction. As a result, the chemical ligands get negligible time to diffuse to an energetically favorable site. It could also arise due to lack of sufficient energy needed by an atom to move to a proper site in forming the crystallite. The crystallite size determined from the Debye-Scherrer formula from the major peak centered at $2\theta = 28.52°$ was estimated to be about 2.2 nm. Detailed XRD analysis is underway to establish the observations of the varying crystallites with different SHMP concentrations as conferred from the optical spectra.

The stabilizing polymer (SHMP) passivates the surface of the particle as can be inferred from the Fourier transform infrared (FTIR) spectroscopy of the synthesized nanophosphors (Fig. 6). The FTIR spectrum was taken for dialyzed and washed samples in order to remove excess unreacted
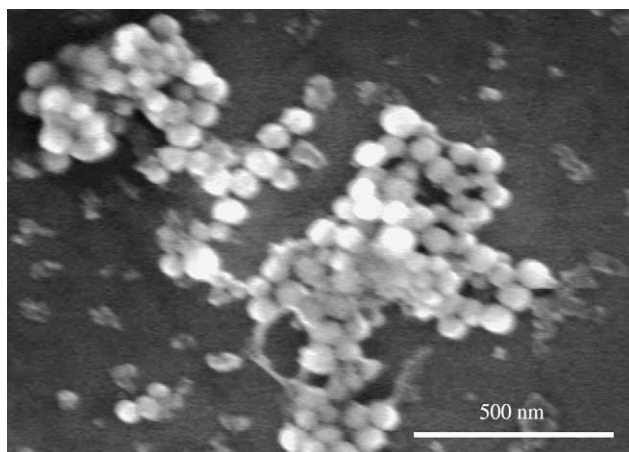
polymers in the solution. The FTIR spectra showed peak at 1636 cm^{-1}, representing the nitrogen–oxygen interaction. The distinct peaks at 1262 and 1086 cm^{-1} are due to phosphorus–oxygen interaction, establishing the presence of covalently bonded phosphates on $ZnS:Mn^{2+}$ nanoparticles. From FTIR spectroscopy, it can be inferred that the stabilizing agent passivates the surface of the particle. The presence of these covalently bonded phosphate groups even
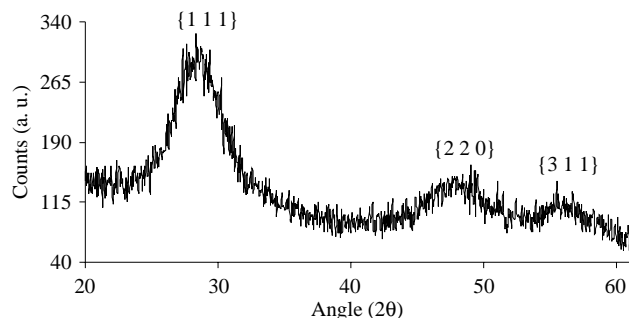

Fig. 5. XRD scan of $ZnS:Mn^{2+}$ nanoparticle, showing broadening of the peaks at {111}, {220} and {311} due to nanocrystalline nature of the crystal. These quantum dots have zinc blende structure. The crystallite size as calculated by Debye-Scherrer formula is 2.2 nm.
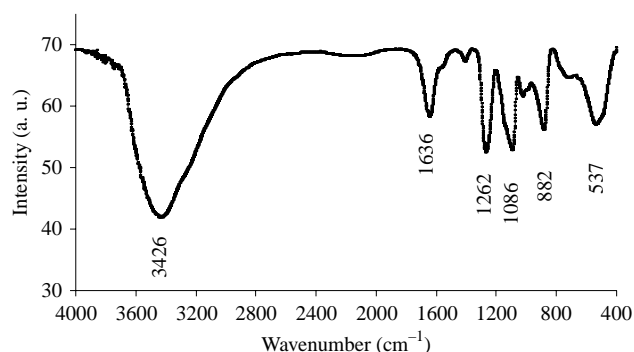

Fig. 4. Scanning electron microscopy of a typical colloidal $ZnS:Mn^{2+}$ showing primary particle size of 60–80 nm which have smooth surfaces due to surface passivation with SHMP.

Fig. 6. FTIR spectra of $ZnS:Mn^{2+}$. Peaks at 1636 cm^{-1} representing nitrogen–oxygen interactions. Peaks at 1262 and 1086 cm^{-1} are due to the phosphorus–oxygen interaction, confirming the presence of covalently bonded phosphates on the nanoparticles $ZnS:Mn^{2+}$.
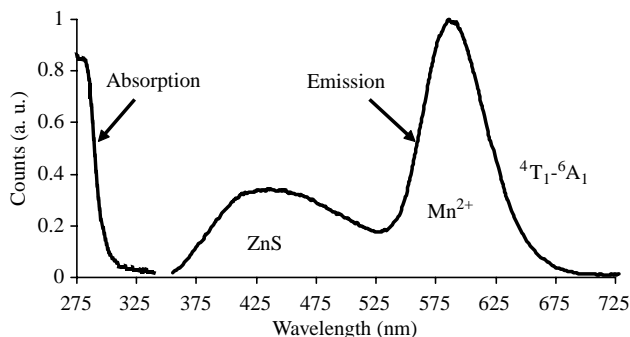
Fig. 7. Normalized UV–Vis absorption and fluorescence emission spectra for manganese doped ZnS nanoparticles. ZnS:Mn^{2+} colloidal nanoparticles have an optical edge at around 285 nm and when excited, glows with orange red color with strong emission at 592 nm. Emission peak at 424 nm is from ZnS nanocrystallites.

after rigorous washing of the colloidal nanoparticles (to remove all unwanted impurities) suggests that SHMP inhibits the growth of particle by steric stabilization. The peak at $882 \, cm^{-1}$ may be due to nitrogen–oxygen interaction, whereas the presence of peak at $537 \, cm^{-1}$ represents either manganese–oxygen or sulfur–oxygen interaction. Passivation with polymers reduces the unsaturated bond density [25], thereby reducing the surface trap sites for non-radiative recombination processes. Thus, capping agents play an important role in the luminosity of the nanophosphors.

ZnS has a direct bandgap of 3.6 eV with an effective energy bandgap of 339 nm at room temperature. On doping zinc sulfide with manganese, the Mn^{2+} ions substitute the Zn^{2+} ions in the ZnS crystal acting as trap sites, where the electrons and holes can be trapped. An electron can undergo photo-excitation process in the host ZnS lattice of nanoparticles and subsequently decay via a non-radiative transition to the $^4T_1$ level to the $^6A_1$ level. The strong emission could be attributed to the radiative decay between these localized states of manganese inside the ZnS bandgap.

The optical absorption spectra show that ZnS:Mn^{2+} colloidal nanoparticles have an absorption edge at around 285 nm and under exposure to ultraviolet light, it glows with an orange red color (emission peaking at 592 nm, Fig. 7). The emission at around 424 nm is typical luminescence of undoped ZnS resulting from the transition of electrons from shallow states near the conduction band to sulfur vacancies present near the valence band.

4. Conclusions

Quantum dots of manganese doped zinc sulfide have been successfully synthesized by a simple precipitation reaction using aqueous route resulting in primary particle sizes of 60–80 nm. The nanoparticles were sterically stabilized using polyphosphates of sodium namely STTP and SHMP. It was established that SHMP was a superior capping agent than STTP. It was observed that the particle sizes are dependant on the amounts of stabilizing agents (SHMP) used during synthesis making it possible to alter the particle sizes by changing the concentrations of stabilizing agents used during synthesis. ZnS:Mn^{2+} has zinc blende structure, as observed by X-ray diffraction, and has a crystallite size of 2.2 nm as calculated by Debye-Scherrer formula. Under UV exposure, the colloidal suspension or powder of ZnS:Mn^{2+} glows with an orange red luminescence peaking at around 590 nm.

ZnS:Mn^{2+} nanoparticles find applications as phosphor layers for futuristic flat panel displays. Minor modifications in the electrolyte composition (replacing manganese ions with ions of silver and copper) result in phosphors emitting in the blue and green region, respectively, such that the photoluminescence in the primary colors of red, blue and green is obtained. By proper surface treatment of doped zinc sulfide nanoparticles, selective attachment to cell walls of specific bacteria can be achieved for use as biolabels akin to cadmium selenide (CdSe) nanocrystals. Work on these lines is currently perused and preliminary results show certain degree of selectivity is possible [26].

References

[1] P.W. Cyr, M. Tzolov, M.A. Hines, I. Manners, E.H. Sargent, G.D. Scholes, Quantum dots in a metallopolymer host: studies of composites of polyferrocenes and CdSe nanocrystals, J. Mater. Chem. 13 (2003) 2213–2219.

[2] H. Fendler, F.C. Meldrum, The colloid chemical approach to nanostructured materials, Adv. Mater. 7 (1995) 607–632.

[3] N. Lopez, T.V.W. Janssens, B.S. Clausen, Y. Xu, M. Mavrikakis, T. Bligaard, J.K. Norskov, On the origin of the catalytic activity of gold nanoparticles for low-temperature CO oxidation, J. Catal. 223 (2004) 232–235.

[4] A.P. Alivisatos, Semiconductor clusters, nanocrystals, and quantum dots, Science 271 (1996) 933–937.

[5] T. Ahmadi, Z.L. Wang, T.C. Green, A. Henglein, M.A. El-Sayed, Shape-controlled synthesis of colloidal platinum nanoparticles, Science 272 (1996) 1924–1926.

[6] D. Yelin, D. Oron, S. Thiberge, E. Moses, Y. Silberberg, Multiphoton plasmonresonance microscopy, Opt. Express 11 (2003) 1385–1391.

[7] A.J. Hoffman, G. Mills, H. Yee, M.R. Hoffmann, Q-sized cadmium sulfide: synthesis, characterization, and efficiency of photoinitiation of polymerization of several vinylic monomers, J. Phys. Chem. 96 (1992) 5546–5552.

[8] J. Dutta, H. Hofmann, Self-organization of colloidal nanoparticles in: H.S. Nalwa (Ed.), Encyclopedia of Nanoscience and Nanotechnology, American Scientific Publishers, California, 2004, pp. 617–640.

[9] K. Mallik, M. Mandal, N. Pradhan, T. Pal, Seed mediated formation of bimetallic nanoparticles by UV irradiation: a photochemical approach for the preparation of core–shell type structures, Nano Lett. 1 (2001) 319–322.

[10] J.H. Yao, K.R. Elder, H. Guo, M. Grant, Theory and simulation of Ostwald ripening, Phys. Rev. B 47 (1993) 14110–14125.

[11] W.G. Becker, A.J. Bard, Photoluminescence and photoinduced oxygen adsorption of colloidal zinc sulfide dispersions, J. Phys. Chem. 87 (1983) 4888–4893.

[12] S.C. Ghosh, M.K. Hossain, C. Thanachayanont, J. Dutta, Manganese doped zinc sulphide nanophosphors, Proceedings of the Second NRCT-KOSEF Workshop on Electronic Materials and Device Processing, Taejong, Korea, 12–15 January 2004 (in press).

[13] M. Wang, L. Sun, X. Fu, C. Liao, C. Yan, Synthesis and optical properties of ZnS:Cu(II) nanoparticles, Solid State Commun. 115 (2000) 493–496.

[14] T. Yamamoto, S. Kishimoto, S. Iida, Materials design for p-Type ZnS with blue Ag emission by triple-codoping method, Phys. Status Solidi 229 (2002) 371–375.

[15] S.C. Ghosh, C. Thanachayanont, J. Dutta, Studies on zinc sulphide nanoparticles for field emission devices, Proceedings of the First ECTI Annual Conference (ECTI-CON 2004), Pattaya, Thailand, 13–14 May 2004, pp. 145–148.

[16] L.G. Wang, S.J. Pennycook, S.T. Pantelides, The role of the nanoscale in surface reactions: CO_2 on CdSe, Phys. Rev. Lett. 89 (2002) 0755061–0755064.

[17] P. Johne, H. Kisch, Photoreduction of carbon dioxide catalysed by free and supported zinc and cadmium sulphide powders, J. Photochem. Photobiol. A 111 (1997) 223–228.

[18] Ch.-H. Fischer, J. Lilie, H. Weller, L. Katsikas, A. Henglein, Photochemistry of colloidal semiconductors 29. Fractionation of CdS sols of small particles by exclusion chromatography, Ber. Bunsenges, Phys. Chem. 93 (1989) 61–64.

[19] R.N. Bhargava, D. Gallagher, X. Hong, A. Nurmikko, Optical properties of manganese-doped nanocrystals of ZnS, Phys. Rev. Lett. 72 (1994) 416–419.

[20] D. Gallagher, W.E. Heady, J.M. Racz, R.N. Bhargava, Homogeneous precipitation of doped zinc sulfide nanocrystals for photonic applications, J. Mater. Res. 10 (1995) 870–876.

[21] I. Yu, T. Isobe, M. Senna, Optical properties and characteristics of ZnS nano-particles with homogeneous Mn distribution, J. Phys. Chem. Solids 57 (1996) 373–379.

[22] R. Vacassy, S.M. Scholz, J. Dutta, C.J.G. Plummer, R. Houriet, H. Hofmann, Synthesis of controlled spherical zinc sulfide particles by precipitation from homogeneous solutions, J. Am. Ceram. Soc. 81 (1998) 2699–2705.

[23] S.M. Scholz, R. Vacassy, J. Dutta, H. Hofmann, M. Akinc, Mie scattering effects from monodispersed ZnS nanospheres, J. Appl. Phys. 83 (1998) 7860–7866.

[24] Minutes of the Philadelphia Meeting December 28, 29, 30, 1926. Phys. Rev. 29 (1927) 350–373.

[25] D.F. Underwood, T. Kippeny, S.J. Rosenthal, Ultrafast carrier dynamics in CdSe nanocrystals determined by femtosecond fluorescence upconversion spectroscopy, J. Phys. Chem. B 105 (2001) 436–443.

[26] H.C. Warad, S.C. Ghosh, C. Thanachayanont, J. Dutta, Highly luminescent manganese doped ZnS quantum dots for biological labeling, SmartMat-'04, International Conference on Smart Materials, Smart/Intelligent Materials and Nanotechnology, Chiang Mai, Thailand, 1–3 December 2004, pp. 203–207.